Electronic Supplementary Information

for

Fluorescence assay for alkaline phosphatase based on ATP hydrolysis-triggered dissociation of cerium coordination polymer nanoparticles

Chuanxia Chen,*[a] Qun Yuan,[b] Pengjuan Ni,[a] Yuanyuan Jiang,[a] Zhenlu Zhao[a] and Yizhong Lu*[a]

[a] School of Materials Science and Engineering, University of Jinan, Jinan 250022, China

[b] Shandong Center for Disease Control and Prevention, Jinan 250014, China

* Corresponding author.

E-mail address: mse_chencx@ujn.edu.cn, mse_luyz@ujn.edu.cn

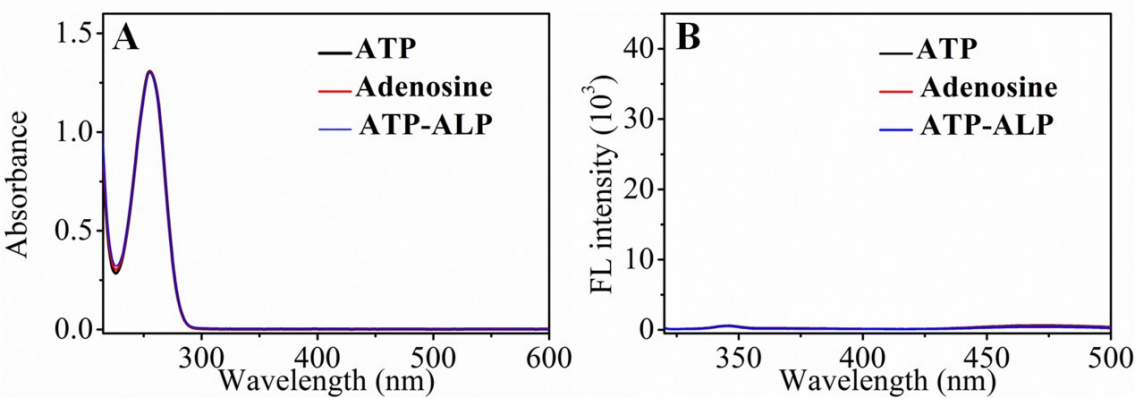

Fig. S1 (A) UV-vis spectra and (B) fluorescence emission spectra monitoring ALP-mediated dephosphorylation reaction of ATP. There is no difference in the spectra between ATP (substrate) and adenosine (product). ATP: 0.1 mM, adenosine: 0.1 mM, ALP: 100 mU/mL.

Table S1 quantum yield of the lanthanide cerium complex

Sample	Integrated emission intensity (I)	Abs. at 310 nm (A)	Refractive index of solvent (η)	Quantum Yield [*a]
Quinine sulfate	4760469.5	0.0311	1.33	0.54 (known)
CPN sample	885662	0.0466	1.33	0.067

[*a] The quantum yield of the CPNs was measured by comparing the integrated photoluminescence intensities and the optical densities with the reference quinine sulfate. The quinine sulfate (literature QY=0.54) was dissolved in 0.1 M H_2SO_4 (refractive index (η) of 1.33) and the CPNs was dissolved in ultrapure water (η=1.33).

$$QY = QY_R \times \frac{I}{I_R} \times \frac{A_R}{A} \times \frac{\eta^2}{\eta_R^2}$$

Where QY is the quantum yield, *I* is the measured integrated emission intensity, η is the refractive index, and A is the optical density. The subscript R refers to the reference fluorophore of known quantum yield.

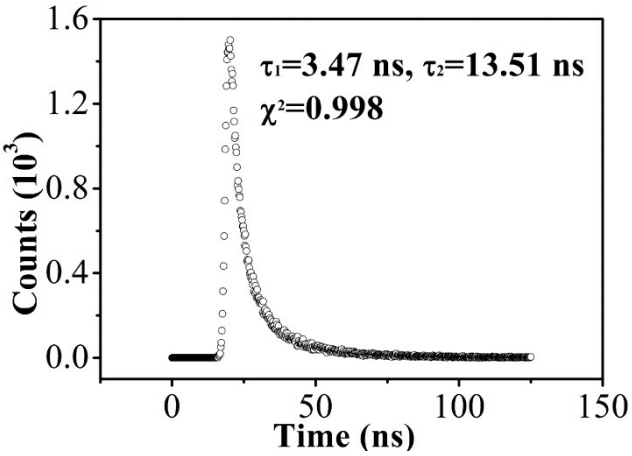

Fig. S2 Time-resolved fluorescence decay spectrum of the lanthanide cerium complex.

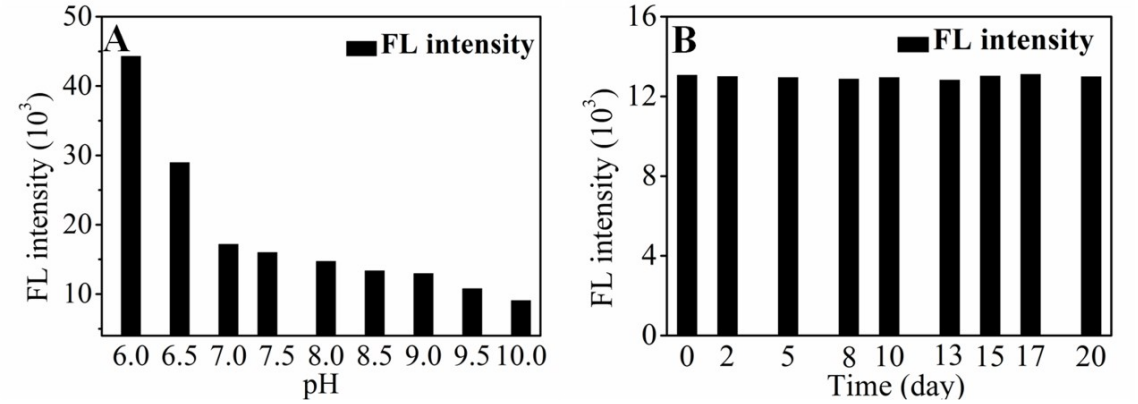

Fig. S3 (A) Effect of pH value on the FL intensity of purified Ce^{3+}-ATP-Tris CPNs. (B) Fluorescence intensity of purified Ce^{3+}-ATP-Tris CPNs in 20 days.

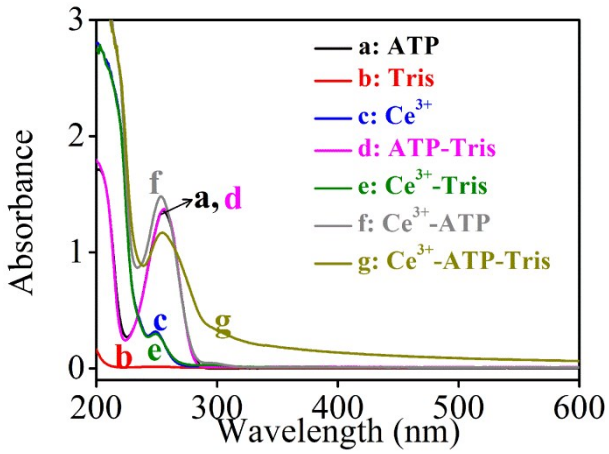

Fig. S4 UV-vis absorption spectra of the ATP solution, Tris-HCl solution, Ce^{3+} solution, ATP-Tris solution, Ce^{3+}-Tris solution, Ce^{3+}-ATP solution and Ce^{3+}-ATP-Tris CPN solution. Cerium nitrate: 0.4 mM, ATP: 0.1 mM, Tris-HCl: 4 mM (pH 7.4).

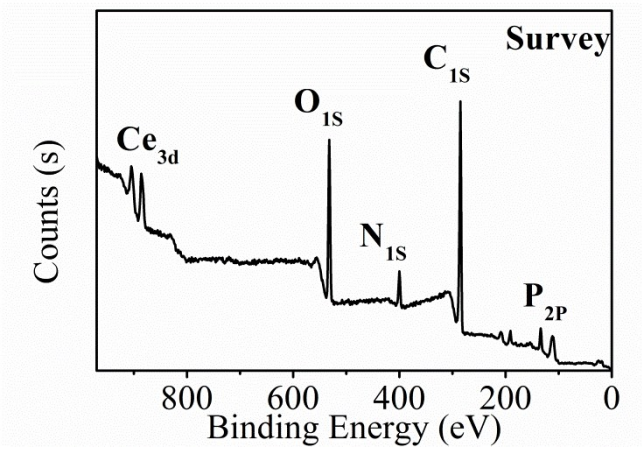

Fig. S5 XPS survey spectra of the as-prepared lanthanide cerium complex.

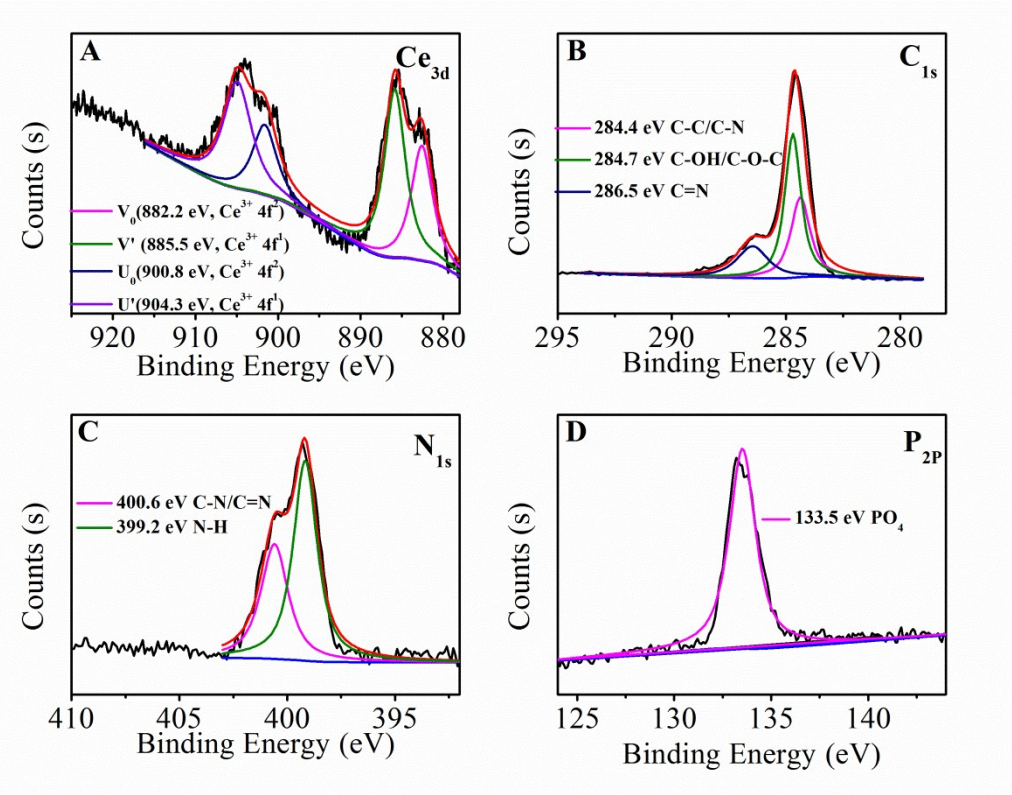

Fig. S6 High-resolution (A) Ce_{3d}, C_{1s}, $N_{1s}$and P_{2p} peaks of the lanthanide cerium complex.

Table S2 Comparison of the current work with other reported methods for the detection of ALP

Method	Sensing system	LOD (mU/mL)	Detection range (mU/mL)	Ref.
Electrochemistry	Ferrocene-based substrate	0.4	1–1000	1
Electrochemistry	CdSe nanoparticles	2	2–25	2
Chemiluminescence	CSPD substrate	0.01	0.01–10	3
Colorimetry	AuNPs/ATP	10	100–600	4
	AuNPs/ATP/Ca^{2+}	3.5	5–100	
	AuNPs/ATP/Pb^{2+}	0.1	0.2–20	
Colorimetry	AuNPs/ATP	8000	8000–5×10^5	5
Colorimetry	AgNPs/ATP	1000	—	6
Colorimetry	Redox active nanoceria	0.04	0.04–2	7
Colorimetry	Cu-MOF/PPi	0.19	1–34	8
Fluorometry	PPECO2-Cu^{2+}	~20	~0–1200	9
Fluorometry	Cu^{2+}-DNA/AgNPs	0.005	0.03–3	10
Fluorometry	AuNCs	0.002	0.02–50	11
Fluorometry	CdS QDs	0.5	0–50	12
Fluorometry	Chalcone derivative	0.15	0–150	13
Fluorometry	SiNPs	0.2	0.2–30	14
Fluorometry	Calcein-Ce^{3+}	0.023	0.1–0.4, 0.4–1.2	15
Fluorometry	CoOOH/NGQDs	0.07	0.1–5	16
Fluorometry	Ce^{3+}-ATP-Tris	0.09	0.1–10	This work

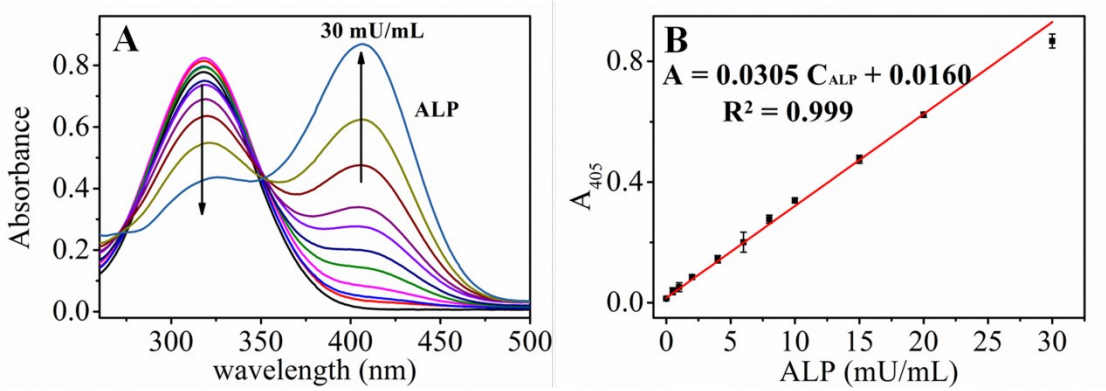

Fig. S7 (A) The UV-vis absorption spectra of the standard pNPP-based colorimetric sensing system in the presence of different concentrations of ALP (0 to 30 mU/mL). (B) Calibration curve of ALP measured by the pNPP-based standard chromogenic method. The detection of ALP activities by pNPP-based standard chromogenic method was proceeded as follows. 200 μL of ALP with different concentrations and 200 μL of pNPP (5 mM) were successively added into 600 μL of DEA-HCl buffer (1.0 M, 0.5 mM $MgCl_2$, pH 9.8). The solution was incubated at 37 °C for 30 min, and was subsequently terminated by adding 100 μL of 2 M Na_2CO_3. The absorption spectra of the resulted solution were measured after being brought to room temperature for 20 min. The absorbance at 405 nm were recorded and analyzed.

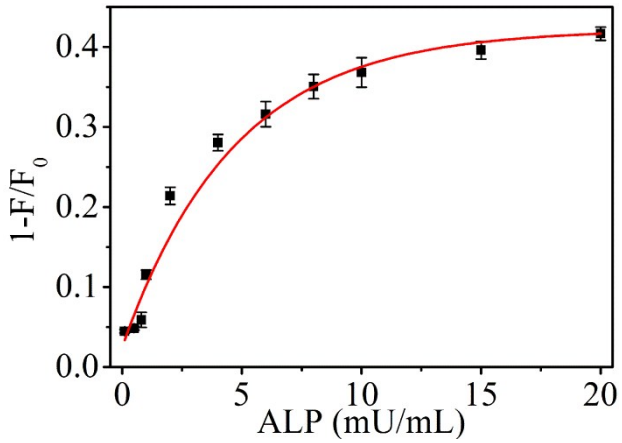

Fig. S8 The calibration curve for ALP detection in diluted serum (5%). Error bars represent the standard deviations (n = 3). Experimental conditions: 0.4 mM Ce^{3+}-ATP-Tris CPNs, pH 9.0 (10 mM Tris-HCl), 37 °C, 60 min.

REFERENCE

1 S. Goggins, C. Naz, B. J. Marsh and C. G. Frost, *Chem. Commun.*, 2015, **51**, 561.

2 H. Jiang and X. Wang, *Anal. Chem.*, 2012, **84**, 6986.

3 J. S. Blum, R. H. Li, A. G. Mikos and M. A. Barry, *J. Cell. Biochem.*, 2001, **80**, 532.

4 C. M. Li, S. J. Zhen, J. Wang, Y. F. Li and C. Z. Huang, *Biosens. Bioelectron.*, 2013, **43**, 366.

5 W. Zhao, W. Chiuman, J. C. Lam, M. A. Brook and Y. Li, *Chem. Commun.*, 2007, DOI: 10.1039/b705335e, 3729.

6 H. Wei, C. Chen, B. Han and E. Wang, *Anal. Chem.*, 2008, **80**, 7051.

7 A. Hayat, B. Gonca and S. Andreescu, *Biosens. Bioelectron.*, 2014, **56**, 334.
8 C. Wang, J. Gao, Y. Cao and H. Tan, *Anal. Chim. Acta*, 2018, **1004**, 74.
9 Y. Liu and K. S. Schanze, *Anal. Chem.*, 2008, **80**, 8605.
10 J. L. Ma, B. C. Yin, X. Wu and B. C. Ye, *Anal. Chem.*, 2016, **88**, 9219.
11 H. Liu, M. Li, Y. Xia and X. Ren, *ACS Appl. Mater. Interfaces*, 2017, **9**, 120.
12 N. Malashikhina, G. Garai-Ibabe and V. Pavlov, *Anal. Chem.*, 2013, **85**, 6866.
13 Z. Song, R. T. K. Kwok, E. Zhao, Z. He, Y. Hong, J. W. Y. Lam, B. Liu and B. Z. Tang, *ACS Appl. Mater. Interfaces*, 2014, **6**, 17245.
14 J. Sun, T. Hu, C. Chen, D. Zhao, F. Yang and X. Yang, *Anal. Chem.*, 2016, **88**, 9789.
15 C. Chen, J. Zhao, Y. Lu, J. Sun and X. Yang, *Anal. Chem.*, 2018, **90**, 3505.
16 J. Liu, D. Tang, Z. Chen, X. Yan, Z. Zhong, L. Kang and J. Yao, *Biosens. Bioelectron.*, 2017, **94**, 271.